Incidence of PV Module Rated Power Tolerances on PV System Energy Production

G. Cipriani*, V. Di Dio*, A. Marcotulli*, R. Miceli*‡

* Department of Energy, Information engineering and Mathematical models (DEIM), University of Palermo, VialedelleScienze, Building 9, Palermo, Italy

(giovanni.cipriani@unipa.it, vincenzo.didio@unipa.it, andreamarcotulli@gmail.com, rosario.miceli@unipa.it)

‡Corresponding Author; R. Miceli,Department of Energy, Information engineering and Mathematical models, University of Palermo, VialedelleScienze, Palermo 90128, Italy, rosario.miceli@unipa.it

Received: 30.01.2015 Accepted:17.03.2015

Abstract-Discussing the electrical energy production of a PV system realized by PV modules with a large range of tolerance for the rated power values is the aim of this paper. In particular, the paper shows how the incidence of tolerance can be significant, in terms of output power reduction, when the PV system works in partial shading condition. For this issue, using a tool developed for this purpose, several simulations have been run, which consider different tolerance values for the module rated power and different shading patterns for the PV array. The authors quantify the peak power values of the different system configurations, showing the importance of the choice of modules with reduced tolerance and providing useful indications for designers of photovoltaic systems as well. The proposed methodology is useful to calculate the payback time of PV system for each module choice.

Keywords- Manufacturing tolerances, mismatch, I-V characteristics, PV module defects.

Nomenclature

V	module output voltage [V]
I_L	photo-generated current [A]
I_0	reverse saturation current of the diode [A]
q	electric charge of an electron [C]
K	Boltzmann constant [J/K]
T	junction temperature
γ	shape factor
R_s	series resistance [Ω]
A	completion factor
N_{cs}	number of cells connected in series per module
G	radiation
STC	Standard Test Conditions
G^{ref}	irradiance at standard test conditions
T^{ref}	the PV module temperature at STC
μ_{Isc}	temperature coefficient of the short-circuit current [A/K]
μ_{Voc}^{ref}	open circuit voltage temperature coefficient given by the manufacturer [V/K]
V_{oc}^{ref}	open circuit voltage at STC [V]
I_{sc}^{ref}	current at short-circuit at STC [A]
V_{mp}^{ref}	voltage at the maximum power point STC [V]
I_{mp}^{ref}	current at the maximum power point at STC [A]
V_0^{ref}	reverse saturation current of the diode at STC [A]
E_G	is the material band-gap energy [eV]
m	number of modules in series
n	number of string in parallel
I_k	current flowing in a series of m modules
V_{string}	voltage string
K_ε	statistical factor representing the deviation from the rated power of the individual modules
$\varepsilon_{\%}(+)$	positive tolerances limits
$\varepsilon_{\%}(-)$	negative tolerances limits
r	random number
P_N	PV module rated power [W]
V_{mp}	voltage value at the maximum power point [V]
I_{mp}	current value at the maximum power point [A]
P_{mp}	power value at the maximum power point [W]
P_{ideal}	output power value calculated not taking into consideration the tolerance [W]
$\Delta P[W]$	difference between P_{ideal} and P_{mp} [W]
$\Delta P_{\%}$	percentage variation between P_{ideal} and P_{mp}

1. Introduction

In the field of photovoltaics much of the scientific research, at the moment, is aimed at identifying new materials that can be used in photovoltaic (PV) conversion.

The new materials under consideration can and must ensure: higher conversion efficiency and stable electric parameters for their lifetime. At the same time the technical production process to realize the PV cells and modules must not be overly complex, in order to obtain products immune from defects deriving from their manufacture, given that the lifespan and reliability of PV modules are highly influenced by defects which originate during the manufacturing process.

Up to now, many varieties of materials have been used in the PV industry but crystalline silicon has had the most significant market share.

As regards this material, the single cells, obtained by slicing a crystalline silicon wafer, are connected in series and in parallel in order to reach higher voltage and current values. The PV cells array, obtained in this way, is successively encapsulated to create a PV module, which on average lasts more than 20 years. The encapsulation process additionally guarantees robustness to withstand mechanical load, protection from atmospheric agents and humidity and electrical insulation for people's safety.

The module is made up of different layers. The upper layer is made of a glass surface which provides mechanical rigidity while allowing solar radiation to penetrate and illuminate the cells. The intermediate layer is constituted by the cells array and the outer layer is commonly realized by a composite plastic sheet. The layers are finally sealed by an encapsulant (EVA is frequently used) and an aluminum framework is commonly added.

This manufacturing process can cause some defects which can be classified considering both the time interval in which they occur and their level of severity.

Considering the first classification, we can find defects that are immediately discernible and others that occur and worsen during the module lifespan (EVA browning, delamination, etc.) [1, 2]. Considering the second classification: critical, medium and slight defects can occur.

Accurate quality controls reveal defects of the first and second class. Moreover these controls ensure that the modules stack will not be rejected by the buyer. An efficient quality assurance can identify slight defects, reducing the rated parameters tolerance of the module, in particular the tolerance of the rated power under standard conditions and of the conversion efficiency. However the modules currently available in the market have rated electrical characteristics that can vary within ±10% of rated power.

This paper evaluates the performances of PV system, giving particular attention to the tolerance effects, using a simulation tool based on a 4 lumped parameters model that was specially developed for this purpose. Several simulations have been developed which consider different tolerances for the module rated power and different shading patterns for the PV array. The results have allowed us to quantify the peak power value of the different system configurations, showing the importance of the choice of modules with reduced tolerance and with the aim of providing useful indications for designers of photovoltaic systems as well.

2. PV Module Mathematical Model

The distributed parameters equivalent circuit is one of the best representation of the PV cell operating mode. This model takes into account both the material resistances, which limit the PV cell current and voltage output values, and the structural defects, introducing resistive elements distributed throughout the PV cell volume [3–5]. In literature [4,5]we can find proposals of several simplifications of the model, but due to it's complexity, the distributed parameters model has been supplanted by the simplified lumped models, which can have varying numbers of diodes and resistances [4, 6–9].

From an electrical point of view, an ideal PV module can be modelled by a current source in parallel with a diode. To increase the precision of the model, several diodes and resistances in series or in parallel with the current source have been added. The four lumped parameters model [4] has been chosen for consideration in this paper because it offers a good compromise between computational cost and accuracy [10].

Regarding the former, when running simulations of PV systems having elevated installed power with complexity in terms of layout and noteworthy surface of the PV modules (so that each module can function in different temperature [11] and radiation conditions), the four lumped parameters model is particularly useful due to its reduced computational burden.

In the latter, the deviancy values between the I-V curves obtained by the four lumped parameters model and the manufacturer I-V characteristics curves, both in the maximum power point (MPP) and close to it, are comparable with the approximations connected to the data provided by the manufacturers, which have been used for the model's implementation. The PV module output voltage V can be expressed by [12, 13]:

$$V = \frac{\gamma KT}{q}\ln\left(\frac{I_L - 1}{I_0} + 1\right) - IR_s \qquad (1)$$

whereI_L is the photo-generated current, $I_0$is the reverse saturation current of the diode, $q$is the electric charge of an electron (1.602 × 10 − 19 C), K is the Boltzmann constant

(1.381 × 10 − 23 J/K), T is the junction temperature, γ is the shape factor, $R_s$is the series resistance and V is the output voltage. The shape factor is a measure of cell imperfection and is related to the completion factor A by the following relation:

$$\gamma = AN_{cs} \tag{2}$$

whereN_{cs} is the number of cells connected in series per module.

The Eq. (1) has four unknown parameters (γ, R_s,I_L, I_0). Two, $\gamma$and R_s, can be considered constant while $I_L$varies in function of solar radiation and cell temperature and I_0in function of temperature only. The photo-generated current, at any radiation $G$and temperature$T$, can be calculated as a function of the photo-generated current in reference condition I_L^{ref} (STC - Standard Test Conditions) with the following equation [3, 9]:

$$I_L = \frac{G}{G^{ref}}\left[I_L^{ref} + \mu_{Isc}\left(T - T^{ref}\right)\right] \tag{3}$$

where:

- G^{ref} is the irradiance at standard test conditions ($1000W/m^2$);
- T^{ref} is the PV module temperature at STC (298.15 K);
- μ_{Isc} is the temperature coefficient of the short-circuit current, given by the manufacturer.

The reverse saturation current$I_0$is related to the temperature and the saturation current can be estimated at reference conditions with the following expression [9]:

$$I_0 = I_0^{ref}\left(\frac{T}{T^{ref}}\right)^3 \exp\left[\frac{qE_G}{KA}\left(\frac{1}{T^{ref}} - \frac{1}{T}\right)\right] \tag{4}$$

where I_0^{ref} is the saturation current at STC and E_G is the material band-gap energy (1.12 eV for Si, 1.35 eV for GaGs).

In the modules datasheet the manufacturers generally provides information about three characteristic points on the I − V curve in STC: the voltage at open circuit (V_{oc}^{ref}), the current at short-circuit (I_{sc}^{ref}) and the voltage and current at maximum power point (V_{mp}^{ref}, I_{mp}^{ref}) [10]. Several methodologies have been developed in literature to determine the four unknown parameters. In this paper the methodology explained in [10] has been chosen.

In addition, in this paper, for the R_s evaluation a method based on a comparison between the calculated load voltage temperature coefficient value, μ_{Voc}^{ref}, with the same coefficient provided by the manufacturer has been adopted. In order to calculate the μ_{Voc}^{ref}coefficient, the following equations have been implemented [10]:

$$\mu_{Voc}^{ref} = \frac{\gamma K}{q}\left[\ln\left(\frac{I_{sc}^{ref}}{I_0^{ref}}\right) + \frac{T^{ref}\mu_{Isc}}{I_{sc}} - \left(3 + \frac{qE_G}{KAT^{ref}}\right)\right] \tag{5}$$

The adopted algorithm starts from an arbitrary initial value of resistance$R_s$in order to calculate μ_{Voc}^{ref} value and then compares it with the one provided by the manufacturer. In order to minimize the error on μ_{Voc}^{ref}, a PI controller is employed as estimator. The algorithm has been implemented in Matlab/Simulink environment using a few predefined and optimized Matlab/Simulink libraries blocks, ensuring a high execution speed.

After several iterations, the algorithm calculates theR_s final value. The block diagram of the algorithm used for the$R_s$determination, implemented in Matlab/Simulink environment, is depicted in Fig.1a. The desired μ_{Voc}^{ref} value has been achieved by setting the proportional and integral PI constants which then define the number of iterations and the final error. The *VocCoeff.temp.block* depicted in Fig.1a operates as shown in Fig.1b. It is drawn from Matlab/Simulink environment. In particular, the μ_{Voc}^{ref} value is obtained starting from R_s and using equations (6), (7) and (5) [10].

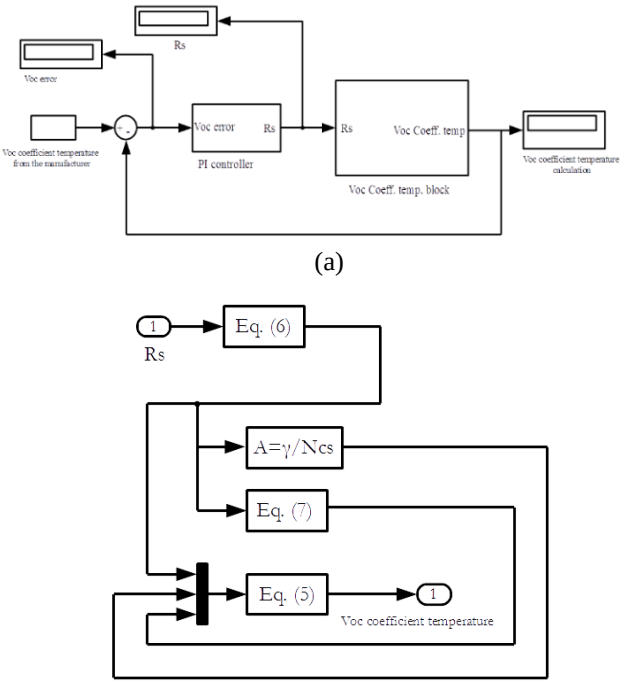

(a)

(b)

Fig. 1. Block diagram of the algorithm for $R_s$determination.

$$\gamma = \frac{q\left(V_{mp}^{ref} + I_{mp}^{ref}R_s - V_{oc}^{ref}\right)}{KT^{ref}\ln\left(1 - \frac{I_{mp}^{ref}}{I_{sc}^{ref}}\right)} \tag{6}$$

$$I_0^{ref} = I_{sc}^{ref} \exp\left(-\frac{qV_{oc}^{ref}}{\gamma K T^{ref}} \right) \quad (7)$$

Starting from eq. (1), that is useful simulate a single PV module, a tool to predict the working conditions of an entire PV system has set up. The tool allows to depict the I–V characteristic of a PV system constituted of several series connected modules and several parallel connected strings, even if the modules are characterized by different values of rated power tolerance and are under different environmental conditions (radiation and temperature). Moreover all the PV system elements have to be represented by a mathematical expression (each PV module, bypass diode, blocking diode).

Taking into consideration *m* modules series connected we have:

$$I_1 = \ldots = I_i = \ldots = I_m = I_k \quad (8)$$

where I_k is the current flowing through the *m* modules.

Neglecting the voltage drop on the cables and diodes, the string voltage is given by the sum of the voltages across each module as following:

$$V_{string} = \sum_{i=1}^{m} V_i(I_k) \quad (9)$$

where $V_i(I_k)$ is the voltage across the i-th string module.

Indeed, in case of series connected modules, if the load current exceeds the short-circuit current of the shaded module (or with a worst characteristic), that module is reverse biased and it is seen as a passive load from the remaining modules of the series. The negative voltage across the shaded module forward biases its bypass diode reducing the amount of local heating at the shaded area and avoiding damage to the module.

To identify the operating point of the string, the behavior of the by-pass diode has been assimilated to that one of an ideal diode.

Considering the bypass diode and the equation (1), $V_i(I_k)$can be expressed as follows:

$$V_i(I_k) = \begin{cases} 0 & I_k \geq I_{sc,i} \\ \frac{\gamma K T_i}{q} \ln\left(\frac{I_{L,1} - I_k}{I_{0,i}} + 1 \right) - I_k R_s & I_k < I_{sc,i} \end{cases} \quad (10)$$

where $I_{L,i}$ is the photo-generated current, $I_{0,i}$ the reverse saturation current and $I_{sc,i}$ the short-circuit current of the i-th module. Substituting in (9) the $V_i(I_k)$ term calculated with (10), it can be obtained the operating point of the string.

Dual is the working principle in the case of *n* parallel strings where the blocking diode prevents reverse current flow on strings at lower voltage.In this case, each string have the same voltage across its terminal and the total current is the sum of the currents supplied by each string:

$$V_1 = \ldots = V_j = \ldots = V_n = V_k \quad (11)$$

Considering the presence of blocking diode in series with each string, the current of the j-th string can be expressed as:

$$I_j(V_k) = \begin{cases} 0 & V_k \geq V_{oc,j} \\ I_j & V_k < V_{oc,j} \end{cases} \quad (12)$$

where $V_{oc,j}$ is the open circuit voltage of the j-th string. Substituting in (11) the $I_j(V_k)$ term calculated with (12), it can be obtained the operating point of the whole PV field.

3. Manufacturing Tolerances

The technological process to manufacture silicon solar cells and to assemble the PV modules are very complicated so that several defect can affect the modules. A lot of these defects are easily identifiable by the naked eye like [14, 15]: bubbles, chips or cracks in cells, corrosion of cell connections, delamination of the solar cell back sheet, partially shaded cells and non-uniform sealant in the frame [16–18].

Other defects can derive from impurities in the silicon material of which the cell is made. These impurities result in a reduction of the output current from the defective cell, which could operate under reverse bias determining an hot-spots [14, 15, 19, 20].

The defects significantly affect the performance of each PV module. That is why the manufacturers have to assign a tolerance on the rated value of the PV module power output. As a result the models of PV modules have to take into account the different power output values.

To model the impact of the tolerances on the I-V and P-V characteristics of the PV modules it is necessary to consider that the manufacturers normally provides three typical points of the rated I-V characteristic obtained under standard conditions (short-circuit current, open circuit voltage, maximum power with its corresponding current and voltage); but the tolerance is normally assigned only for maximum power [21].

The approach used in this paper allow to obtain the model of the PV module by assuming that the effect of tolerance determines an alteration of the characteristic analogous to that one originated by a variation of the solar radiation incident on the module surface.

As manufacturing tolerances are due to statistically independent and random causes, therefore, for a generic sample of PV modules, we suppose the maximum power deliverable from each module as a random variable with normal or Gaussian probability distribution. This assumption

is theoretically supported by the Lindeberg and Lévy central limit theorem. The statistical dispersion of I−V characteristics is taken into account by multiplying the expression of the photo-generated current (4) by a statistical factorK_ε representing the deviation from the rated power of the individual modules, whose expression is function of positive$\varepsilon_{\%}(+)$ and negative $\varepsilon_{\%}(-)$ tolerances limits:

$$K_\varepsilon = f\,[\varepsilon_{\%}(+),\varepsilon_{\%}(-)] \qquad (13)$$

Fig. 2 shows the I − V and P − V curves corresponding to the rated characteristic ($\varepsilon_{\%}$=0) and to a power tolerance of 10% ($\varepsilon_{\%}$=10)for a 200 W PV module obtained using the model previously explained. A power tolerance of 10% is one of the higher value that can be found in the PV commercial modules datasheet.

Thanks to a Matlab environment implementation, theK_ε factor is calculated generating a random number *r* from a normal distribution with the following expression:

$$K_\varepsilon = \frac{r}{P_N} \qquad (14)$$

where$P_N$is the PV module rated power.

The method used to get the random number *r*, both in case of symmetrical and asymmetrical tolerance limits, is shown in [12].

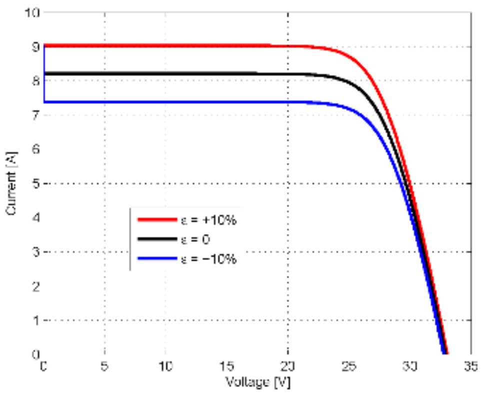

(a)

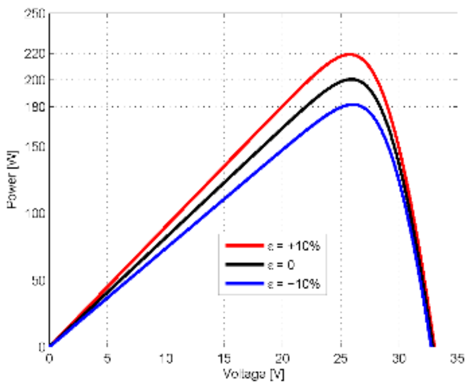

(b)

Fig. 2. I-V and P-V curves corresponding to the rated characteristic ($\varepsilon_{\%}$=0) and to a power tolerance of 10% ($\varepsilon_{\%}$=10) for a 200 W PV module.

4. Simulation Conditions

A typical PV system installed on the roof of an industrial building have been considered to run the simulations. The photovoltaic array configuration taken into account is composed by 9 parallel string each one formed by 22 PV modules connected in series (totalling 198 PV modules). Each module has a rated power of 200 Wp in STC, therefore the cumulative rated power of the PV system is equal to 39,6kWp. The module Kyocera KC200GHT-2 datasheet [21] has been taken into account to calculate the unknown mathematical model parameters.

Several simulation have been developed, considering both different tolerance values for the module rated power and shading conditions for the PV array. The considered tolerance values for the module rated power are equal to ± 5 % and ± 10 %. These values are typical for PV commercial module. In the first simulation (Fig. 3 - pattern 1), that represent a reference for successive performance comparisons, the PV array is considered uniform radiated (800 W/m^2). In the other simulations, plausible obstacles that determines different shading shapes and levels are considered.

800	800	800	800	800	800	800	800	800	800	800	800	800	800	800	800	800	800	800	800	800	800
800	800	800	800	800	800	800	800	800	800	800	800	800	800	800	800	800	800	800	800	800	800
800	800	800	800	800	800	800	800	800	800	800	800	800	800	800	800	800	800	800	800	800	800
800	800	800	800	800	800	800	800	800	800	800	800	800	800	800	800	800	800	800	800	800	800
800	800	800	800	800	800	800	800	800	800	800	800	800	800	800	800	800	800	800	800	800	800
800	800	800	800	800	800	800	800	800	800	800	800	800	800	800	800	800	800	800	800	800	800
800	800	800	800	800	800	800	800	800	800	800	800	800	800	800	800	800	800	800	800	800	800
800	800	800	800	800	800	800	800	800	800	800	800	800	800	800	800	800	800	800	800	800	800
800	800	800	800	800	800	800	800	800	800	800	800	800	800	800	800	800	800	800	800	800	800

Fig. 3. The considered PV array uniform radiated – pattern 1

In particular, the effect of passing clouds above the PV roof (Fig. 4 - pattern 2a, 2b and 2c), the shading caused by a high and narrow building (Fig. 5 - pattern 3) and vice versa in the third case, by a low and wide building (Fig. 6 - pattern 4) have been simulated.

To take into account the different shading level produced by the considered various obstacles, for the shading conditions caused by a passing cloud, the solar irradiance was 800 W/m^2, 400 W/m^2 and 300 W/m^2 respectively for fully irradiated modules, shaded modules under the peripheral areas of the cloud and shaded modules under the central areas of the cloud. Moreover three different position of the cloud above the PV roof have been considered (see Fig. 4).

For the other two cases, the solar irradiance was equal to 800 W/m^2 for fully irradiated modules and 200 W/m^2 for shaded modules (see Fig. 5 and Fig.6).

The solar radiation levels for each module (indicated by a rectangle) of the PV array are indicated in Fig. 3, 4, 5 and 6.

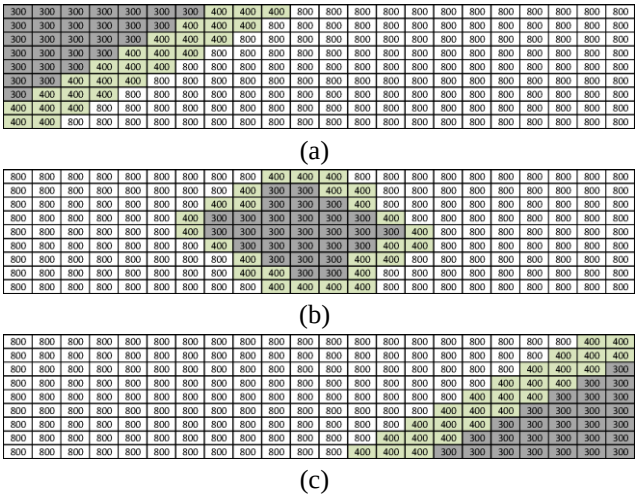

Fig. 4. The considered PV array in shading conditions caused by a passing cloud – pattern 2a, 2b, 2c.

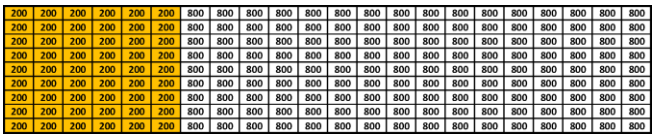

Fig. 5. The considered PV array in shading conditions caused by a high and narrow building – pattern 3.

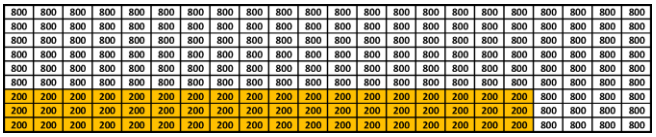

Fig. 6. The considered PV array in shading conditions caused by a low and wide building – pattern 4.

Table 1 summarizes all the simulated PV system working conditions.

Table 1. Simulated PV system working conditions.

N.	pattern	$\varepsilon_{\%}(+)$	$\varepsilon_{\%}(-)$	N.	pattern	$\varepsilon_{\%}(+)$	$\varepsilon_{\%}(-)$
1	1	0	0	13	2.c	0	0
2	1	10	-5	14	2.c	10	-5
3	1	10	-10	15	2.c	10	-10
4	1	5	0	16	2.c	5	0
5	2.a	0	0	17	3	0	0
6	2.a	10	-5	18	3	10	-5
7	2.a	10	-10	19	3	10	-10
8	2.a	5	0	20	3	5	0
9	2.b	0	0	21	4	0	0
10	2.b	10	-5	22	4	10	-5
11	2.b	10	-10	23	4	10	-10
12	2.b	5	0	24	4	5	0

5. Simulation Results

The set up simulation tool has been used, in all the working conditions of Table 1, to depict the P-V characteristics curves of the PV system and to obtain the results summarized in Table 2.In the first column, the output current values of the PV system obtained, for each simulation, in the maximum power point (I_{mp}) are reported. The other columns report respectively: the PV system output voltage values (V_{mp}), output power values (P_{mp}) and the output power values (P_{ideal}) calculated not taking into consideration the tolerance effects.The last two columns report the absolute and percentage differences, in terms of power output, respect to P_{ideal}, for each pattern.

Table 2. Maximum power point values obtained for each simulation

N.	I_{mp}[A]	V_{mp}[V]	P_{mp}[A]	P_{ideal} [W]	ΔP[W]	ΔP%
1	54,77	576,87	31597,27	31597,27		
2	54,78	579,26	31730,65		133,39	0,42
3	53,90	583,20	31434,85		-162,42	-0,51
4	55,08	577,32	31797,25		199,98	0,63
5	48,58	412,77	20050,84	20050,84		
6	48,50	413,57	20059,35		8,51	0,04
7	47,98	412,32	19780,84		-270,01	-1,35
8	48,83	412,62	20149,38		98,53	0,49
9	54,63	382,90	20919,49	20919,49		
10	54,21	383,93	20814,15		-105,34	-0,50
11	54,19	381,06	20650,92		-268,57	-1,28
12	54,83	383,35	21018,47		98,98	0,47
13	48,58	412,77	20050,84	20050,84		
14	45,79	437,23	20020,54		-30,31	-0,15
15	48,00	413,60	19852,18		-198,66	-0,99
16	48,82	412,68	20145,40		94,55	0,47
17	54,76	419,64	22979,83	22979,83		
18	54,93	421,27	23140,65		160,82	0,70
19	53,99	423,29	22851,26		-128,57	-0,56
20	55,08	419,83	23123,86		144,03	0,63
21	41,08	575,02	23623,39	23623,39		
22	41,04	577,39	23695,45		72,05	0,31
23	40,35	581,61	23466,06		-157,34	-0,67
24	41,32	575,43	23775,69		152,30	0,64

Particularly Fig. 7 shows the P-V curves depicted for pattern 1 in the foreseen four different rated power tolerances of the modules. The curves of Fig. 7 obtained not taking into consideration the tolerance for the module rated power, which represent a reference for performance comparisons, is depicted with a magenta trace.Fig. 8 to 12 show the same characteristics curves with regards to pattern 2, 3 and 4.

The curves depicted in Fig. 7 highlight relevant differences in the points close to the maximum power point. The maximum difference between the ideal condition and the investigated conditions is equal to + 0,63%. Whereas the maximum difference between two investigated conditions is equal to 1,14%. Moreover the maximum difference between the ideal condition and the investigated conditions and the maximum difference between two investigated conditions are equal to -1,35 and 1,84, -1,28 and 1,76, -0,99 and 1,46 respectively for pattern 2a, 2b and 2c of figures 8, 9 and 10. The corresponding values related to pattern 3 and 4 of figures 11 and 12 are 0,70 and 1,26, -0,67 and 1,31.

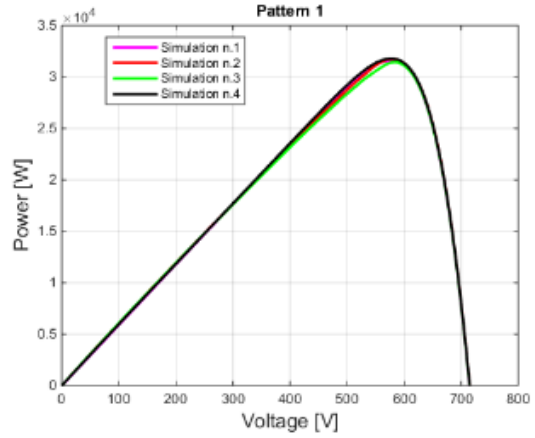

(a)

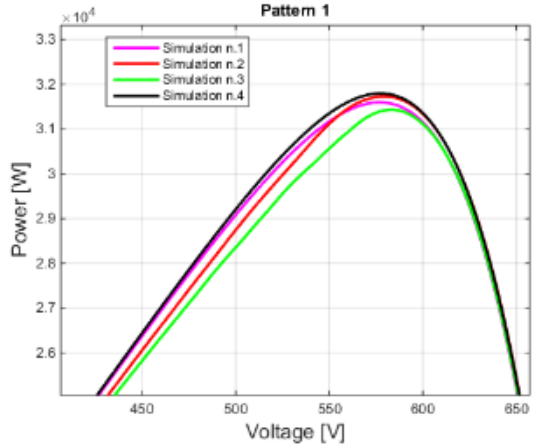

(b)

Fig. 7. P-V curves depicted for pattern 1 in the foreseen four different rated power tolerances of the modules a) entire curves; b) points close to MPP.

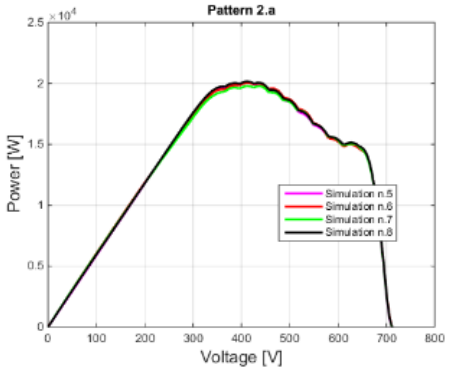

(a)

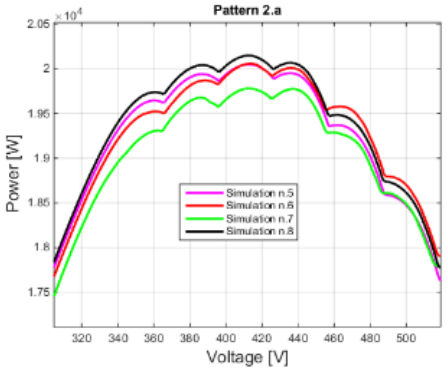

(b)

Fig. 8. P-V curves depicted for pattern 2a in the foreseen four different rated power tolerances of the modules a) entire curves; b) points close to MPP.

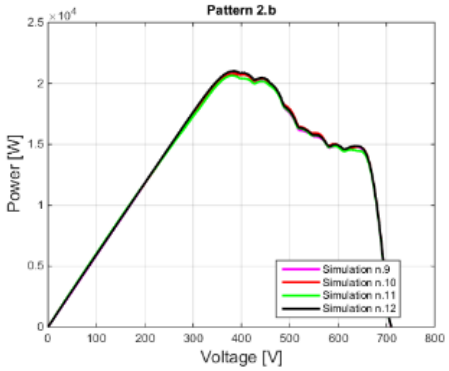

(a)

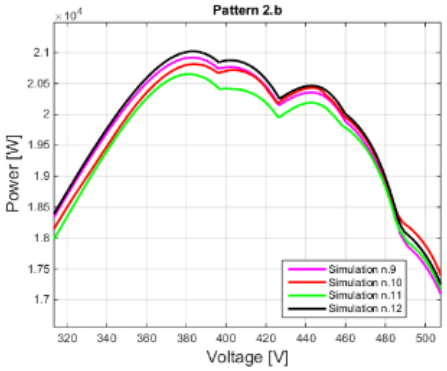

(b)

Fig. 9. P-V curves depicted for pattern 2b in the foreseen four different rated power tolerances of the modules a) entire curves; b) points close to MPP.

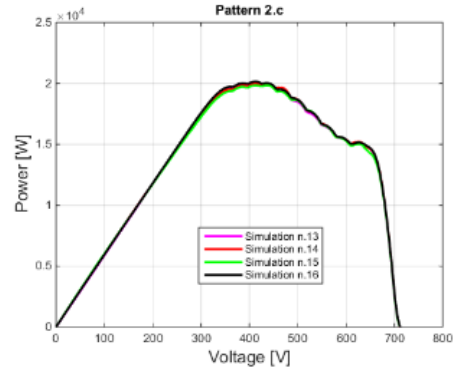

(a)

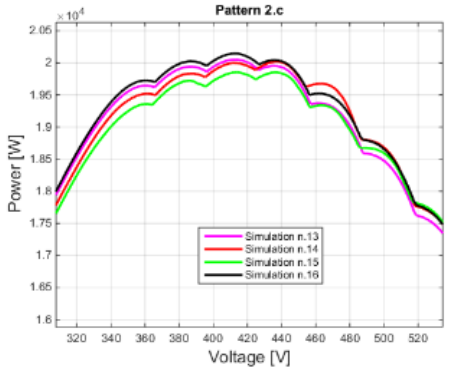

(b)

Fig. 10. P-V curves depicted for pattern 2c in the foreseen four different rated power tolerances of the modules a) entire curves; b) points close to MPP.

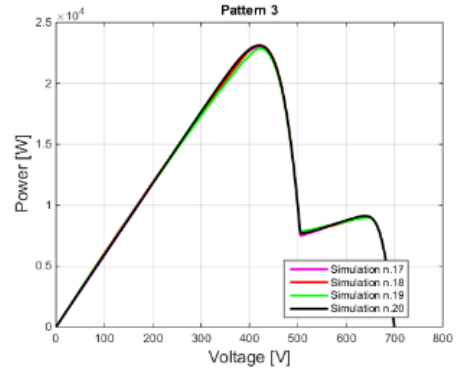

(a)

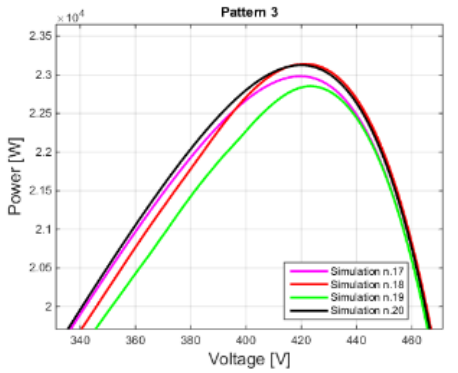

(b)

Fig. 11. P-V curves depicted for pattern 3 in the foreseen four different rated power tolerances of the modules a) entire curves; b) points close to MPP.

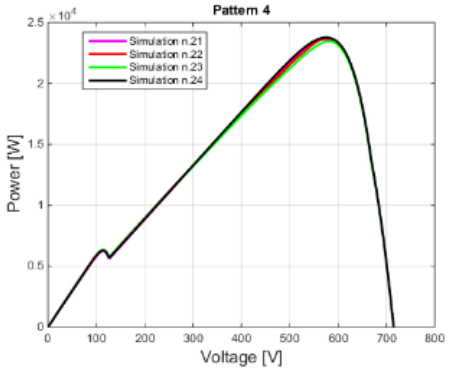

(a)

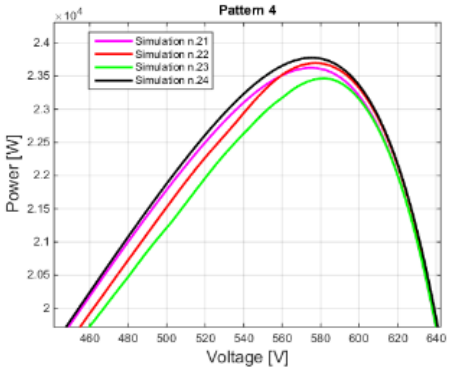

(b)

Fig. 12. P-V curves depicted for pattern 4 in the foreseen four different rated power tolerances of the modules a) entire curves; b) points close to MPP.

The resulting deductions are summarized in Table 2. The data allow us to conclude that the presence of the tolerance values for the module rated power amplifies the mismatch effect due to the shading conditions. In some cases the difference between two investigated conditions reach 1,84%.

6. Conclusion

The present manufacturing processes used for the most common PV module available on the market are complex and may often cause several kinds of defects. This defects, which can be classified considering both the time interval in which they occur and their level of severity, can determine the rejection by the buyer of entire modules stack. To avoid this occurrence an accurate quality control has to be assured. Moreover an efficient quality assurance can identify slight defects, reducing the rated parameters tolerance of the module, in particular the tolerance of the rated power under standard conditions and of the conversion efficiency. However the modules currently available in the market have rated electrical characteristics that can vary within ±10% of rated power. Often this data is neglected. It is, instead, an indicator of possible defects or difference in the production processes and responsible of considerable reductions in the electricity production of photovoltaic plants.

This paper evaluates the performances of PV system, giving particular attention to the tolerance effects, using a simulation tool based on a 4 lumped parameters model that was specially developed for this purpose.

Several simulation have been developed considering different tolerance values for the module rated power (typical for PV commercial modules) and different shading conditions for the PV array.

The tolerance effect, for a generic plant of PV modules, has been considered supposing the maximum power deliverable from each module as a random variable with normal or Gaussian probability distribution.

The different shading conditions consider plausible obstacles that determines different shading shapes and levels for the same PV system. In particular, the effect of passing clouds above the roof, the shading caused by a high and narrow building and vice versa in the third case, by a low and wide building have been simulated.

Simulations have allowed us to quantify the peak power value of the different shading conditions, showing differences between the ideal condition and the investigated conditions equal to -1, 35% and differences between two investigated conditions equal to 1, 84%.

In conclusion, the present paper demonstrates the importance of the choice of modules with reduced tolerance and delivers useful indications for designers of photovoltaic systems. Indeed, the proposed methodology allows to determine the differences in power production due to the use of modules having different tolerance values and, therefore, to calculate the payback time for each module that can be chosen.

The proposed methodology is also applicable to photovoltaic systems working in partial shading conditions, for which the effect of manufacturing tolerances can be particularly significant.

Acknowledgements

This publication was partially supported by the PON PON04a2_H "i-NEXT" Italian research program. This work was realized with the contribution of SDES (Sustainable Development and Energy Savings) Laboratory – UNINETLAB - University of Palermo.

References

[1] S. Kaplanis and E. Kaplani, "Energy performance and degradation over 20 years performance of BP c-Si PV modules," Simulation Modelling Practice and Theory, vol. 19, 2011, pp. 1201–1211.

[2] M.A. Munoz, M.C. Alonso-Garca, N. Vela, and F. Chenlo, "Early degradation of silicon PV modules and guaranty conditions," Solar Energy, vol. 85, 2011, pp. 2264–2274.

[3] A. Luque and S. Hegedus, Handbook of photovoltaic science and engineering, John Wiley & Sons, 2011.

[4] T.U. Townsend, "A method for estimating the long-term performance of direct-coupled photovoltaic systems," University of Wisconsin-Madison, 1989.

[5] M. Wolf and H. Rauschenbach, "Series resistance effects on solar cell measurements," Advanced energy conversion, vol. 3, 1963, pp. 455–479.

[6] R. Chenni, M. Makhlouf, T. Kerbache, and A. Bouzid, "A detailed modeling method for photovoltaic cells," Energy, vol. 32, 2007, pp. 1724–1730.

[7] V. Lo Brano, A. Orioli, G. Ciulla, and A. Di Gangi, "An improved five-parameter model for photovoltaic modules," Solar Energy Materials and Solar Cells, vol. 94, 2010, pp. 1358–1370.

[8] F. Spertino and J.S. Akilimali, "Are Manufacturing I-V Mismatch and Reverse Currents Key Factors in Large Photovoltaic Arrays?," Industrial Electronics, IEEE Transactions on, vol. 56, Nov. 2009, pp. 4520–4531.

[9] M.G. Villalva, J.R. Gazoli, and E.R. Filho, "Modeling and circuit-based simulation of photovoltaic arrays," Power Electronics Conference, 2009. COBEP '09. Brazilian, 2009, pp. 1244–1254.

[10] G. Cipriani, V. Di Dio, D. La Cascia, R. Miceli, and R. Rizzo, "A novel approach for parameters determination in four lumped PV parametric model with operative range evaluations," International Review of Electrical Engineering, vol. 8, 2013, pp. 1008–1017.

[11] R. Siddiqui and U. Bajpai, "Deviation in the performance of solar module under climatic parameter as ambient temperature and wind velocity in composite climate," International Journal of Renewable Energy Research, vol. 2, 2012, pp. 486–490.

[12] G. Cipriani, V. Di Dio, A. Marcotulli, and R. Miceli, "Manufacturing Tolerances Effects on PV Array Energy Production," Renewable Energy Research and Applications (ICRERA), 2014 International Conference on, 2014, pp. 1–6.

[13] V. Di Dio, D. La Cascia, R. Miceli, and C. Rando, "A mathematical model to determine the electrical energy production in photovoltaic fields under mismatch effect," Clean Electrical Power, 2009 International Conference on, 2009, pp. 46–51.

[14] J. Coello, J.L. Galindo, M. Carames, and R. Carreño, "Quality control during the supply of PV modules: fundamental key to guarantee the profitability of PV installations," 23rd European Solar Energy Conference, 1-5 September 2008, Valencia, Spain, 2008.

[15] M. Sander, B. Henke, S. Schweizer, M. Ebert, and J. Bagdahn, "PV module defect detection by combination of mechanical and electrical analysis methods,"

Photovoltaic Specialists Conference (PVSC), 2010 35th IEEE, 2010, pp. 1765–1769.

[16] C.E. Chamberlin, P. Lehman, J. Zoellick, and G. Pauletto, "Effects of mismatch losses in photovoltaic arrays," Solar energy, vol. 54, 1995, pp. 165–171.

[17] S. Shirzadi, H. Hizam, and N.I.A. Wahab, "Mismatch losses minimization in photovoltaic arrays by arranging modules applying a genetic algorithm," Solar Energy, vol. 108, 2014, pp. 467–478.

[18] E. Suresh Kumar and B. Sarkar, "Investigation of the common quality and reliability issues in the photovoltaic panels," Energy Efficient Technologies for Sustainability (ICEETS), 2013 International Conference on, 2013, pp. 320–325.

[19] E. Molenbroek, D.W. Waddington, and K. Emery, "Hot spot susceptibility and testing of PV modules," Photovoltaic Specialists Conference, 1991, Conference Record of the Twenty Second IEEE, 1991, pp. 547–552 vol.1.

[20] M. Simon and E.L. Meyer, "Detection and analysis of hot-spot formation in solar cells," Solar Energy Materials and Solar Cells, vol. 94, 2010, pp. 106–113.

[21] KGT200GT PV Module Datasheet, 2007.